Whole transcriptome profiling of placental pathobiology in SARS-CoV-2 pregnancies identifies a preeclampsia-like gene signature

Nataly Stylianou[1], Ismail Sebina[2], Nicholas Matigian[3], James Monkman[4], Hadeel Doehler[1], Joan Röhl[5], Mark Allenby[6], Andy Nam[7], Liuliu Pan[7], Anja Rockstroh[1], Habib Sadeghirad[4], Kimberly Chung[4], Thais Sobanski[1], Ken O'Byrne[1], Patricia Zadorosnei Rebutini[8], Cleber Machado-Souza[9], Emanuele Therezinha Schueda Stonoga[10], Majid E Warkiani[11], Carlos Salomon[12], Kirsty Short[13], Lana McClements[11], Lucia de Noronha[8], Ruby Huang[14], Gabrielle T. Belz[4], Fernando Souza-Fonseca-Guimaraes[4], Vicki Clifton[15], Arutha Kulasinghe[4*].

[1] *Centre for Genomics and Personalised Health, School of Biomedical Sciences, Queensland University of Technology, Brisbane, QLD 4102, Australia*
[2] *QIMR Berghofer Medical Research Institute, Herston, Queensland 4006, Australia*
[3] *QCIF Bioinformatics, St Lucia, QLD 4102, Australia*
[4] *Frazer Institute, Faculty of Medicine, The University of Queensland, Brisbane, QLD 4102, Australia.*
[5] *Faculty of Health Sciences and Medicine, Bond University, Queensland, Australia*
[6] *BioMimetic Systems Engineering Lab, School of Chemical Engineering, University of Queensland (UQ), St Lucia, QLD, Australia*
[7] *Nanostring Technologies, Inc, Seattle, WA, USA*
[8] *Postgraduate Program of Health Sciences, School of Medicine, Pontifícia Universidade Católica do Paraná´ -PUCPR, Curitiba, Brazil.*
[9] *Postgraduate Program in Biotechnology Applied in Health of Children and Adolescent, Instituto de Pesquisa Pelé Pequeno Príncipe, Faculdades Pequeno Príncipe, Curitiba, Brazil*
[10] *Department of Medical Pathology, Clinical Hospital, Universidade Federal do Paraná´ -UFPR, Curitiba, Brazil.*
[11] *School of Life Sciences & Institute for Biomedical Materials and Devices, Faculty of Science, University of Technology Sydney, NSW, Australia.*
[12] *Exosome Biology Laboratory, Centre for Clinical Diagnostics, University of Queensland Centre for Clinical Research, Royal Brisbane and Women's Hospital, Faculty of Medicine, The University of Queensland, Brisbane, Australia.*
[13] *School of Chemistry and Molecular Biosciences, Faculty of Science, The University of Queensland, St Lucia QLD 4067, Australia.*
[14] *School of Medicine, College of Medicine, National Taiwan University, Taipei, Taiwan.*
[15] *Mater Medical Research Institute – University of Queensland, Brisbane, Australia.*

*Corresponding author: Dr Arutha Kulasinghe, Frazer Institute, Faculty of Medicine, The University of Queensland. 37 Kent Street, Woolloongabba, Queensland 4012, Australia. E: Arutha.kulasinghe@uq.edu.au

Abstract

In recent years, pregnant people infected with the SARS-CoV-2 virus have shown a higher incidence of "preeclampsia-like syndrome". Preeclampsia is a systematic syndrome that affects 5 -8 % of pregnant people worldwide and is the leading cause of maternal mortality and morbidity. It is unclear what causes preeclampsia, and is characterised by placental dysfunction, leading to poor placental perfusion, maternal hypertension, proteinuria, thrombocytopenia, or neurological disturbances.

In this study, we used whole-transcriptome, digital spatial profiling of placental tissues to analyse the expression of genes at the cellular level between placentae from pregnant participants who contracted SARS-CoV-2 in the third trimester of their pregnancy and those prior to the start of the pandemic. Our focused analysis of the trophoblast and villous core stromal cell populations revealed tissue-specific pathways enriched in the SARS-CoV-2 placentae that align with a pre-eclampsia signature. Most notably, we found enrichment of pathways involved in vascular tension, blood pressure, inflammation, and oxidative stress.

This study illustrates how spatially resolved transcriptomic analysis of placental tissue can aid in understanding the underlying pathogenic mechanisms of SARS-CoV-2 in pregnancy that are thought to induce "preeclampsia-like syndrome". Moreover, our study highlights the benefits of using digital spatial profiling to map the crosstalk between trophoblast and villous core stromal cells linked to pathways involved in "preeclampsia-like syndrome" presenting in pregnant people with SARS-CoV-2.

Introduction

Viral infections during pregnancy can disrupt placental function and predispose pregnant women to several complications including late onset preeclampsia, preterm birth, still birth, and intrauterine foetal demise.[1-3] Recent studies have revealed that a "preeclampsia-like syndrome" develops in pregnant women who have encountered Severe Acute Respiratory Syndrome Coronavirus 2 infection (SARS-CoV-2; coronavirus disease 2019; COVID-19). [4-8] Vasculopathy and inflammation, two pathological features linked to preeclampsia, are heightened in placental tissues from COVID-19 patients.[9] Moreover, some of the clinical features present in COVID-19 patients, such as COVID-19 associated hypertension, endothelial dysfunction, kidney disease, thrombocytopenia, and liver injury, overlap with those observed in preeclampsia.[4,10]

Placental dysfunction is the root cause of preeclampsia, a systemic syndrome that occurs in 5-8% of pregnant people and the leading cause of maternal and perinatal morbimortality in pregnancy.[11,12] Preeclampsia is categorised based on time of symptom detection, with early onset at <34 weeks of gestation, and late onset at >34 weeks.[13] Although the causes are unclear, early onset preeclampsia is associated with poor placentation resulting in downstream placental malperfusion and dysfunction[13,14]. One feature that separates early from late onset preeclampsia is the presence of restricted foetal growth which is less likely to occur with late onset[13,14]. Factors contributing to late onset preeclampsia are thought to stem from maternal pathologies that lead to placental disfunction, such as systemic hypertension and endothelial disfunction that can present with SARS-CoV-2 infection.[13]

The placenta forms the functional interface between the mother and foetus, and is essential for foetal development and growth during gestation.[15] The maternal-foetal interface is comprised of various anatomically distinct sites of immunological contact. These sites include the decidua basalis, where maternal immune cells and decidual stromal cells interact with foetal extravillous trophoblasts; the placental intervillous space, in which circulating maternal immune cells interact with the foetal syncytiotrophoblasts; and the boundary where the parietalis meets the chorion laeve in the chorioamniotic membranes.[16] Other cell types within the maternal-foetal interface include villous cytotrophoblasts, column cytotrophoblasts, fibroblasts, endothelial cells, and Hofbauer cells.[15] Together, these distinct cell types and histological features mediate nutrient and waste exchange, hormone production, protection from pathogens, and maternal immune responses to enable in-utero existence.[16]

We utilised digital spatial whole-transcriptomic analysis of human placental tissue to understand the pathogenic mechanisms of SARS-CoV-2 in pregnancy at the cellular level. Specifically, we focused on elucidating the distinct transcriptional response of the trophoblast and villous core stroma cell populations (endothelial, fibroblast, and immune cells) to SARS-CoV-2, which revealed a number of key pathways underlying SARS-CoV-2 associated "preeclampsia-like syndrome". Understanding the molecular pathways through which a SARS-CoV-2 infection predisposes pregnant people to a "preeclampsia-like syndrome" in pregnancy may contribute to developing new interventions for improved pregnancy outcomes in people with high-risk pregnancies.

Material and Methods

Study Design

The study involved two groups; a SARS-CoV-2 group and a control group. The SARS-CoV-2 group comprised of pregnant unvaccinated participants (n=10) who were COVID-19 symptomatic and confirmed to be positive for SARS-CoV-2 by RT-qPCR (of nasopharyngeal swabs) within their third trimester. Placenta tissue samples from this group were collected during delivery at the Pontificia Universidade Catolica do Paraná (PUCPR), Curitiba, Brazil in accordance with the National Commission for Research Ethics (CONEP) under ethics approval 30188020.7.1001.0020.[17] The control group consisted of historic archived placentae from COVID-negative people (n=10) collected during delivery at the Complexo Hospital de Clínicas, Universidade Federal do Paraná, Curitiba, Brazil between 2016 and 2018. All participants provided written informed consent. The study was ratified by the University of Queensland and Queensland University of Technology Human Research Ethics Committees. The two groups were matched based on maternal age, gestational age, and maternal comorbidities. Placental weight, size, and macroscopic changes were recorded as well as foetal weight, sex, and delivery method. The demographic of the study cohort is shown in Table 1. All placenta samples were examined

histologically by a trained pathologist and representative areas from the centre of the placenta were collected. Two tissue microarrays (TMA) were prepared from the placental samples.

Due to demise of three foetuses from the SARS-CoV-2 group (2 postnatal and 1 in utero), we focused our analysis on the seven placental samples with viable deliveries. Further, nine from ten placenta samples from the control group were analysed due to one sample being of low quality for sequencing.

Table 1: Clinical information of the SARS-CoV-2 and control cohort

Patient De-id.	Group	Sample Code	Participant Age	Gestational Age	Comorbidities	SARS-CoV-2 symptoms/ severity	Fetal sex	Fetal Outcome	Delivery Method	Fetal Weight (grams)	Placental Weight (grams)	Macroscopic observations
20-3594	SARS-CoV-2	2	25-30	30-35	Hypothyroidism and hypertensive disorder in pregnancy	+/+	Male	Preterm	na	2450	448	Infarcts and intervillous thrombosis (<5%)
20-3561	SARS-CoV-2	4	35-40	25-30	Hypothyroidism	+/+	Female	Preterm	C-section	na	245	-
20-3744	SARS-CoV-2	8	25-30	30-35	Gestational diabetes, bipolar disorder, hypothyroidism and syphilis (treated)	+/-	Female	Preterm	C-section	na	412	Infarcts (<5%)
20-5105	SARS-CoV-2	12	25-30	35-40	None	-	Female	Term	C-section	2960	462	-
20-3369	SARS-CoV-2	13	25-30	35-40	Gestational diabetes and hyperthyroidism	+/-	Female	Term	Assisted Vaginal	2600	358	Retroplacental and marginal hematoma, infarcts (<5%)
20-5869	SARS-CoV-2	18	25-30	35-40	None	+/-	Male	Term	C-section	2345	370	-
20-2916	SARS-CoV-2	22	20-25	35-40	None	-	Female	Term	Assisted Vaginal	3030	650	-
16-7859	CONTROL	1	20-25	30-35	Hypothyroidism		Male	Preterm	C-section	1180	270	Placental hypoplasia
18-13016	CONTROL	3	20-25	35-40	Hypothyroidism and hypertension		Female	Preterm	Assisted Vaginal	2223	498	-
16-8315	CONTROL	5	15-20	35-40	Obesity		Female	Term	Assisted Vaginal	3810	514	-
18-4906	CONTROL	9	20-25	25-30	None		Male	Preterm	Assisted Vaginal	1205	248	-
18-14057	CONTROL	10	40-45	30-35	Diabetes, hypertension, bipolar disorder		Male	Preterm	C-section	1650	243	Placental hypoplasia
16-7599	CONTROL	11	25-30	35-40	Gestational diabetes		Male	Term	C-section	3460	480	-
16-3340	CONTROL	15	35-40	35-40	None		Female	Term	C-section	3005	395	-
18-9951	CONTROL	16	20-25	35-40	None		Male	Term	C-section	3690	574	-
16-6144	CONTROL	19	25-30	35-40	None		Male	Term	C-section	3345	394	-

Digital spatial profiling with Nanostring GeoMX platform

TMA slides were stained with fluorescent markers to visualise histological features and cell types. Specifically, CD68 staining identified macrophages, Pan-Cytokeratin (PanCK) identified trophoblasts, vimentin (VIM) identified endothelial and mesenchymal stromal cells, and DAPI identified nuclei (Table 2). With the aid of a trained placental pathologist, an area featuring an anchoring villus, and an area featuring a cluster of terminal villi, were designated as two areas of interest within each placental core. Transcript expression was collected separately for the trophoblasts (PanCK positive cells) and the rest of the villus core stromal cells (villous core stroma; endothelial, stromal, and immune cells; VIM/CD68 positive cells) from either the anchoring or terminal villi of each placental core. TMAs were hybridised using the NanoString Technologies Whole Transcriptome Atlas (WTA) barcoded-probe set (~18,000 genes), before cleaving and collecting the barcodes from each sample by UV light. Probe barcodes were then sequenced and counted using an Illumina® sequencer, then matched to their representative genes before proceeding with normalisation and transcriptomic analysis.

Table 2: Fluorescent markers used to identify areas of interest in placental cores

Stain	Histological feature/ Cell Type
Vimentin (VIM)	Endothelial and stromal cells
Pan-Cytokeratin (PanCK)	Trophoblasts
CD68	Macrophages
SYTO 13	Nuclei

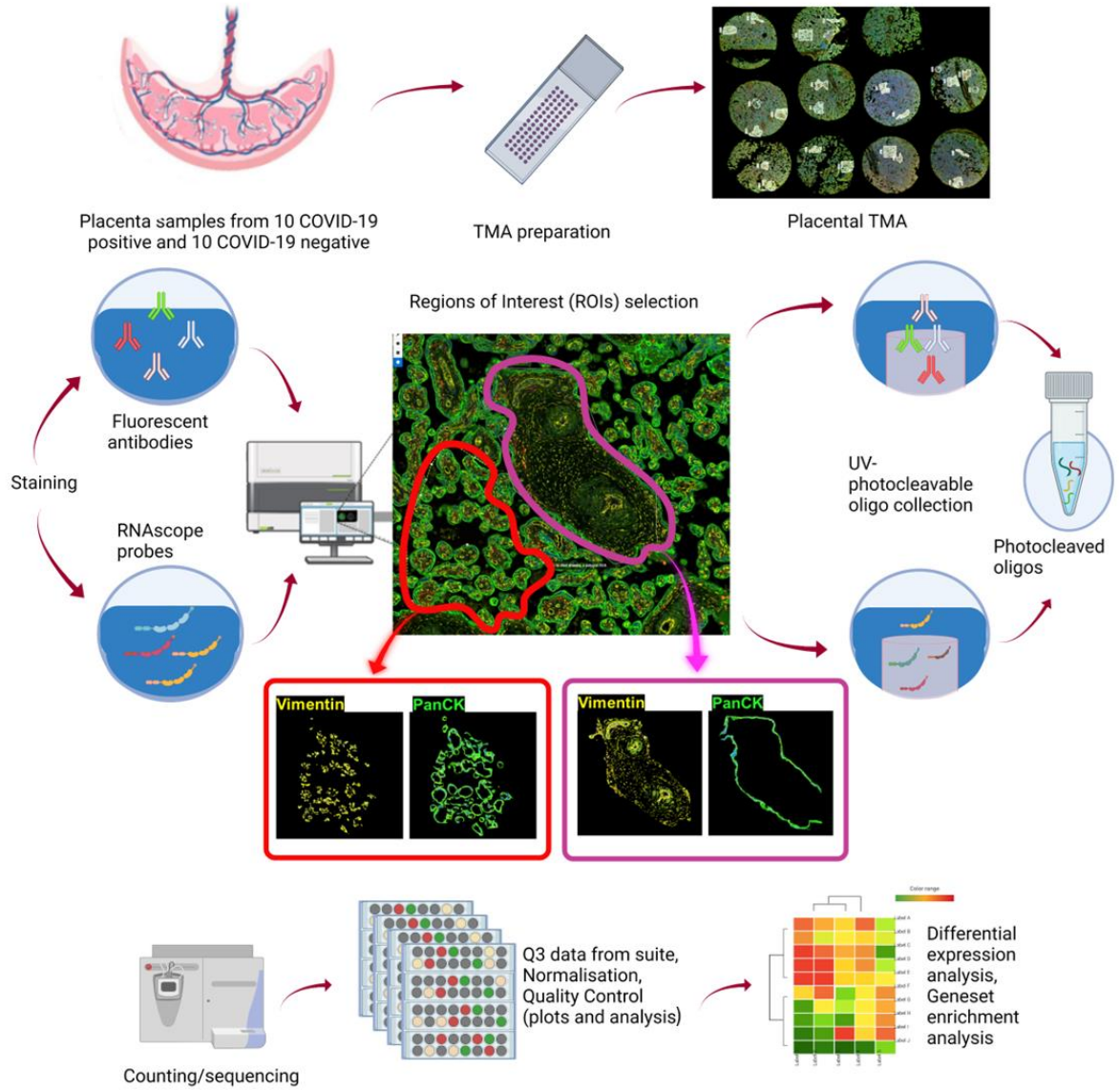

Figure 1: NanoString GeoMX® Workflow. *Placental tissues collected at delivery from the SARS-CoV-2 and control groups were assembled into tissue microarray slides (TMAs) in a randomized order. TMAs were stained with fluorescent markers to differentiate cell types within anchoring and terminal villi. Barcodes were cleaved and collected from each region of interest by UV light. Cleaved barcodes were sequenced and counted using an Illumina® sequencer in preparation for transcriptomic analysis. Data was normalised with RUVSeq before downstream differential expression analysis.*

Data normalisation, differential expression analysis and pathway enrichment analysis

Raw data was normalised to the 134 negative probes in the Human Whole Transcriptome Atlas probe set followed by upper quantile normalisation using the R package RUVseq.[18] Since DSP collected transcriptional data from regions of interest (ROIs) contained either PanCK expressing cells (trophoblasts cells) or VIM/CD68 expressing cells (villous core stroma cells), the normalisation was conducted separately for each cell group prior to downstream analyses. Differential gene expression analysis between SARS-CoV-2 positive and negative groups was performed separately for trophoblasts or villous core stroma containing ROIs using the R package limma.[19] Bayesian adjusted t-statistic method was used where foetal sex and TMA slide number were

considered as co-variants. A fold change of +/-1.5 and $p \leq 0.05$ (adjusted for a false discovery rate (FDR) of 5%) was considered significant. Pathway enrichment analysis was performed using the R package Gene Set Variation Analysis (GSVA) using the "gsva" method for biological pathways obtained from the Molecular Signatures Database (MSigDB, Broad Institute, Human v2022.1).[20] Gene Set enrichment was further clustered and visualised using the R package vissE (vissE parameters: computeMsigOverlap (thresh = 0.25), findMsigClusters (alg = cluster_walktrap, minSize =2)).[21]

Results

Patient characteristics and histopathological characterisation of collected placentae

Placenta cores were obtained immediately following delivery from 7 participants who tested positive for SARS-CoV-2 within 15 days prior to delivery (April 2020, Alpha strain, unvaccinated, median age 28 [24 to 38], median gestational age 37 weeks [28+2 to 38+6]), and 9 participants who did not contract SARS-CoV-2 during their pregnancy (median age 24 [18 to 42], median gestational age 37 weeks [28 to 39]). There were no significant differences observed in placental weight, foetal weight, gestational age, or maternal age between the SARS-CoV-2 and control groups. Within the SARS-CoV-2 group, three out of seven new-borns were delivered pre-term, compared to four out of nine in the control group. Four participants from the SARS-CoV-2 group, and five participants from the control group had recorded comorbidities including hypothyroidism, hyperthyroidism, bipolar disorder, and gestational diabetes mellitus. The placentae from three participants from the SARS-CoV-2 group had macroscopic detection of infarcts (<5%), with one showing intervillous thrombosis, and one with retroplacental and marginal hematoma. Two placentae from the control group displayed placental hypoplasia that led to pre-term delivery. Placental cores from the SARS-CoV-2 group had no detectable SARS-CoV-2 viral load following examination by RNAscope of the SARS-CoV-2 spike mRNA. Enumeration of the cell types within each placental core revealed the SARS-CoV-2 group to have a significantly higher number of CD68 positive immune cells within the terminal villi (mean of 585 cells per sample) compared to the control group (mean of 275 cells per sample, 2.12 mean fold-change, p=0.0218; Figure 2). This was not observed for PanCK expressing or Vimentin expressing cells (Figure 3).

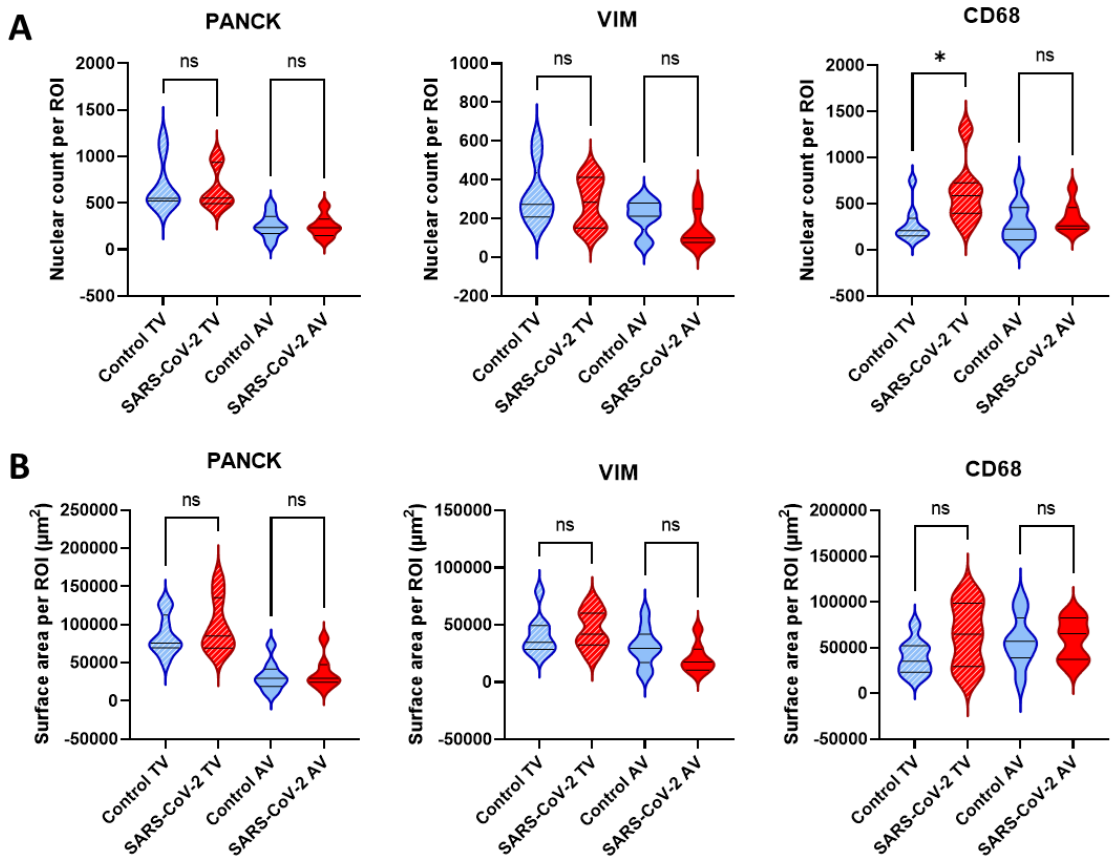

***Figure 2: Cell counts from NanoString GeoMx analysis**: **A)** Nuclear count per region of interest (ROI) at the terminal villi (TV) or anchoring villi (AV) for either PanCK, VIM, or CD68 positive cells. **B)** Fluorescent surface area per ROI (µm²) at the TV and AV containing PanCK, VIM, or CD68 positive cells.*

Terminal and anchoring villi share a transcriptional response to SARS-CoV-2 that is reminiscent of preeclampsia

We first examined whether gene expression from the captured cell populations differed between anchoring and terminal villi in response to SARS-CoV-2. Unsupervised clustering by principal component analysis (PCA) showed clear separation by both PC1 and PC2 dimensions for trophoblasts between the SARS-CoV-2 group and the control group (Figure 3A). Similarly, villous core stroma cells from the SARS-CoV-2 group were clearly separated from the control group by both PC1 and PC2 dimensions (inverse pattern to the clustering seen with the trophoblasts; Figure 3A)). Examination of the differentially expressed genes (± 1.5 fold change, $p<0.05$, Supplemental File 1) between SARS-CoV-2 and control groups showed there was a higher number of differentially expressed genes at the anchoring villi in response to SARS-CoV-2 compared to the terminal villi for both trophoblast and villous core stroma cells (1,791 differentially expressed genes in trophoblasts and 1,139 in villous core stroma cells at the anchoring villi versus 493 in trophoblasts and 601 in villous core stroma cells at the terminal villi; Figure 3B; Supplemental File 1). Closer examination of the differentially expressed genes at the terminal villi and anchoring villi showed high overlap in a cell population specific manner; specifically, 82% of the genes altered in trophoblasts in response to SARS-CoV-2 at the terminal villi were also altered at the anchoring villi, and similarly 76% of genes altered in the villous core stroma cells were shared between the terminal and anchoring villi. There was very minimal overlap in differential gene expression between trophoblasts and villous core stroma cells, highlighting their distinct cell phenotypes and functions (Figure 3B).

To assess commonalities and differences in pathway expression between trophoblasts and villous core stroma cells in response to SARS-CoV-2, we performed pathway enrichment analysis using the Hallmark gene signatures from the molecular signatures database (Human MSigDB v2022.1; Supplemental File 1). Both trophoblasts and villous core stroma cells showed significant activation in a number of pathways associated with preeclampsia and oxidative stress, including oxidative phosphorylation and reactive oxygen species pathways, as well as increase in the PI3K/AKT/mTOR signalling pathway (Figure 3C) [22-24]. Alongside, there was increased enrichment of protein secretion pathways, androgen signalling, cholesterol synthesis and homeostasis, as well as glycolysis and fatty acid metabolism. More specific to trophoblast cells was the significantly positive enrichment of E2F targets, peroxisome pathway, and oestrogen response. Villous core stroma cells showed positive enrichment for immune related pathways, including IL2/STAT5, interferon alpha, interferon gamma, complement, IL6/JAK/STAT3, and inflammatory response pathways. Enrichment of TGFβ, Notch, KRAS, and WNT pathways, alongside angiogenesis, hypoxia and apoptosis pathways were significantly increased in villous core stroma cells. Trophoblasts cells showed a significant reduction in pathways associated with allograft rejection, inflammation, angiogenesis, and KRAS, the latter being the only pathway commonly downregulated between trophoblast and villous core stroma cells. Downregulation in bile acid metabolism, pathways involved in pancreatic beta cells, and spermatogenesis were observed in villous core stroma cells. The epithelial mesenchymal transition pathway, marked by dominance of mesenchymal markers, was positively enriched in mesenchymal villous core stroma cells and negatively regulated in epithelial trophoblast cells.

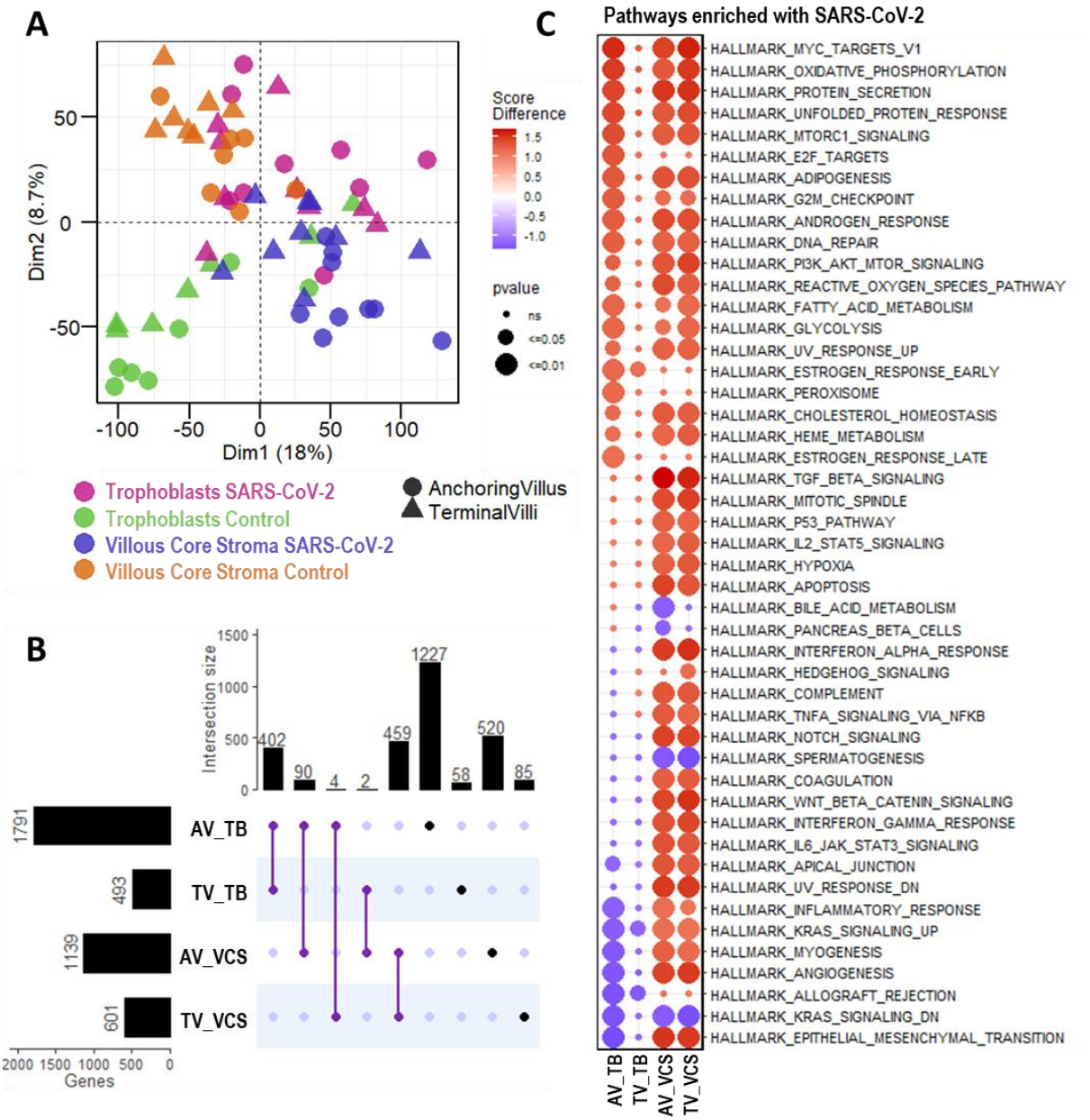

Figure 3: Differential gene expression between anchoring and terminal villi in response to SARS-CoV-2. A) *Principal component analysis of trophoblasts and villous core stroma cells from SARS-CoV-2 and control groups at the anchoring or terminal villi (AV / TV).* ***B)*** *Upset plot showing differential gene expression in trophoblasts and villous core stroma cells from the AV and TV in response to SARS-CoV-2. Fold change +/- 1.5, p-value <= 0.05.* ***C)*** *Differentially enriched pathways in trophoblasts and villous core stroma cells from the AV and TV. Colour gradient refers to score difference in SARS-CoV-2 versus control samples; p-value <= 0.05. TB: Trophoblasts, VCS: Villous Core Stroma Cells.*

Trophoblasts show enrichment of preeclampsia related markers and pathways in response to SARS-CoV-2.

We examined the specific response of trophoblasts cells from the anchoring and terminal villi to SARS-CoV-2. Differential gene expression analysis revealed a combined 1,461 significantly upregulated and 1,339 significantly downregulated genes (Figure 5A; Supplemental File 1). From the upregulated genes, most evident were the immunomodulatory pregnancy specific glycoproteins (PSGs; *PSG1-9* and *PSG11)*, as well as genes from the

Growth Hormone (GH) locus including growth hormone 1 and 2 (*GH1*; *GH2*), Chorionic Somatomammotropin Hormone 2 (*CSH2*), and Chorionic Somatomammotropin Hormone Like 1 (*CSHL1*). Nitric oxide synthase 3 (*NOS3*) was significantly increased with SARS-CoV-2, along with Fms Related Receptor Tyrosine Kinase 1 (*FLT1*), kisspeptin 1 (*KISS1*), Chromogranin A (*CGA*), Growth Differentiation Factor 15 (*GDF15*; also known as macrophage inhibitor cytokine 1; MIC-1), tissue factor pathway inhibitor 2 (*TFPI-2*) and corticotrophin-releasing hormone (*CRH*). Additionally, there was upregulation of placental alkaline phosphatase (*ALPP*) and pregnancy associated plasma protein-A and A2 (*PAPPA* and *PAPPA-2*). Markers involved in synthesis and metabolism of steroid hormones *HSD3B1*, *HSD17B1*, and *CYP19A1* were also upregulated.[25] Genes that were downregulated included osteopontin (*SPP1*/*OPN*), complement component C1Q (*C1QA*/*B*/*C*) and coagulation factor XII (*F13A1*). Additionally, there was downregulation of Caveolin 1 (*CAV1*), a number of collagens (*COL6A1*/*2*, *COL1A1*/*2*, *COL3A1*), decorin (*DCN*),[26] and Delta-like non-canonical Notch ligand 1 (*DLK1*).[27]

In agreement, pathway enrichment analysis of a broader network outside of the Hallmark gene sets (Gene Ontology Biological Pathways [GOBP]), followed by clustering of enriched pathways revealed notable upregulation of pathways related to vascular tension and blood pressure (Figure 5, B and C; Supplemental File 1 and 2). Pathways related to the negative regulation of proliferation and bud formation by *GATA3* were present in cluster 1 (B and C)[28], and pathways related to triglycerides and lipoprotein metabolism were prominent in cluster 4 (B and C). In parallel, cluster 5 (Figure 5, B and C) indicated expression of nitric oxide synthase, a potent vasodilator that regulates vasodilation and angiogenesis during pregnancy[29]. Increase in cell-cell adherence and communication pathways was indicated in cluster 12 (Figure 5, B and C), driven by upregulation of desmosome related markers such as desmoplakin (*DSP*) and desmoglein-2 (*DSG2*). Alongside, there was an increase in pathways related to metal and amino acid transport such as SLC39A8 (*ZIP8*) and SLC11A2 (*DMT1*) as detected in cluster 6 and 9 (Figure 5, B and C). [30] Pathways related to collagen deposition showed reduced expression (clusters 1, Figure 5, D and E), as well as pathways related to vasoconstriction and coagulation (Clusters 6 and 12, Figure 5, D and E). Additionally, complement pathways were decreased alongside MHC related pathways (downregulation of *HLA-A*, *HLA-B*, and *HLA-DRA*) and allograft rejection (clusters 3 and 8, Figure 5, D and E).

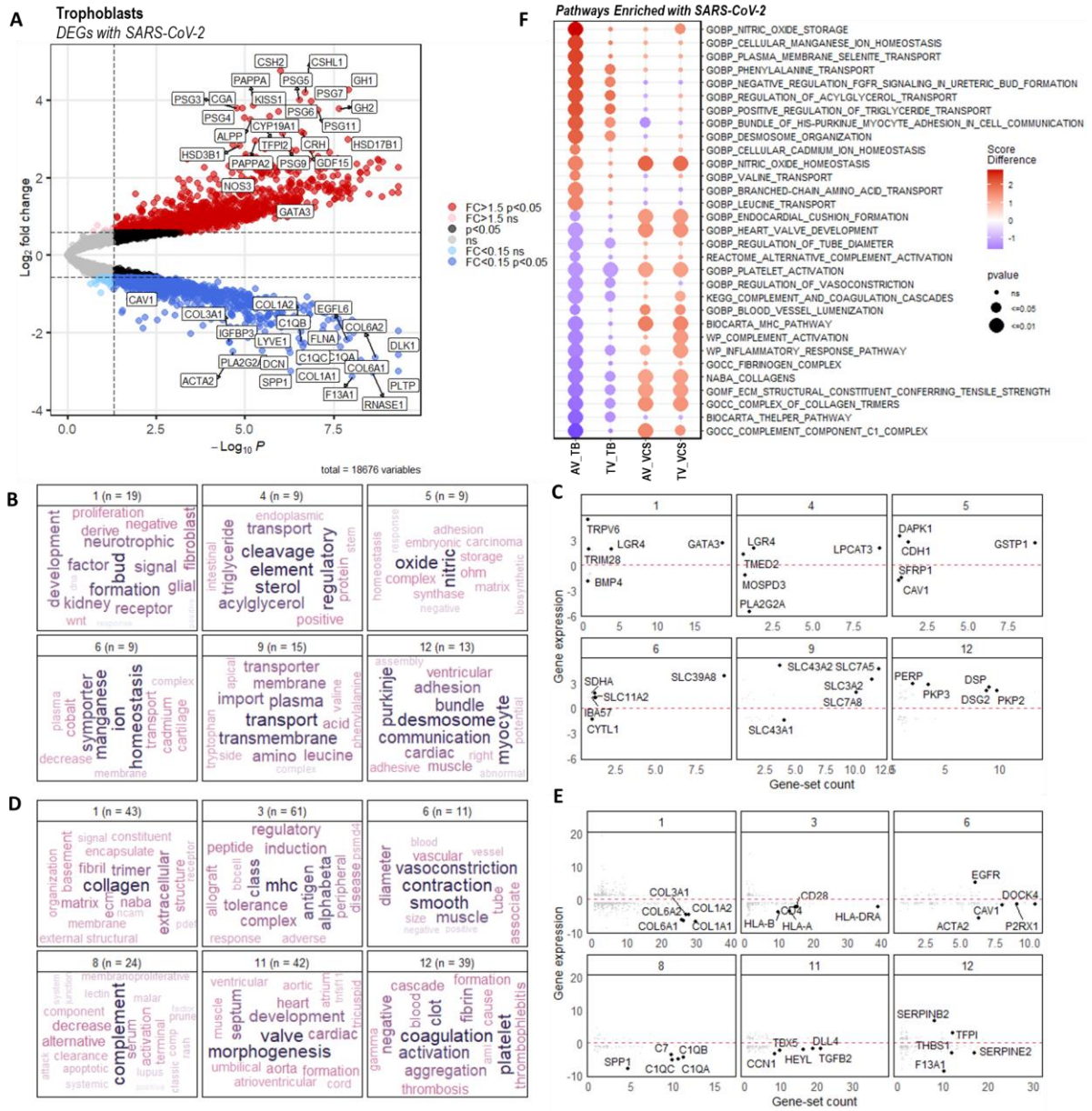

Figure 4: Response of trophoblast cells to SARS-Cov-2. ***A****) Volcano plot of gene expression from trophoblasts in response to SARS-CoV-2. Fold change (FC) +/- 1.5, p-value <= 0.05.* ***B****) Select pathway clusters positively enriched in trophoblasts and* ***C****) the top 5 most common genes within each pathway cluster in C.* ***D****) Select pathway clusters negatively enriched in trophoblasts and* ***E****) the top 5 most common genes within each pathway cluster in D. Number of pathways within each pathway cluster is indicated at the top of each cluster box. Top 20 positively and negatively enriched pathway clusters can be found in Supplemental File 2.* ***F)*** *Enrichment score difference of select pathways from B and D in trophoblasts and villous core stroma cells at the anchoring and terminal villi. Full list of enriched pathways can be found in Supplemental File 1. Colour gradient refers to score difference in SARS-CoV-2 versus control samples; p-value <= 0.05. TB: trophoblasts, VCS: villus core stroma cells, AV: anchoring villi, TV: terminal villi, DEGs: differentially expressed genes.*

Villous core stroma cells show enrichment of preeclampsia related pathways in response to SARS-CoV-2.

We examined the response of the villous core stroma cells at the anchoring and terminal villi to SARS-CoV-2. Differential gene expression analysis revealed villous core stromal cells to have 1,026 significantly upregulated

and 2,697 significantly downregulated genes in response to SARS-CoV-2 shared between the anchoring and terminal villi (Figure 6 A; Supplemental File 1). Among the top upregulated genes were several structural proteins i.e., collagens (*COL3A1*, *COL4A1/2*, *COL15A1*), nidogen-1 (*NID1*), and vimentin (*VIM*). Upregulation of the collagenase inhibitor Alpha-2-microglobulin (*A2M*) was also significant alongside platelet endothelial cell adhesion molecule-1 (*PECAM1*), epidermal growth factor-like domain-containing protein 6 (EGFL6), hypoxia inducing factor 3A (*HIF3A*), and transforming growth factor b1 (*TGFβ-1*). In parallel, osteonectin (*SPARC*), SPARC-Like 1 (*SPARCL1*), Caveolin-1 (*CAV1*), focal adhesion pathway (*FAK*/*PTK2*) and *DLK1* were also upregulated. Additionally, there was upregulation of the PAPPA2 substrates *IGFBP4* and *IGFBP5*, where their interaction leads to increased *IGF2* which was also upregulated in the villous core stroma cells.[31] MHC class I molecules beta-2-microglobulin (*B2M*) and a number of HLA molecules (*HLA-A*/*B*/*E*) were increased, along with monocyte infiltration associated transmembrane signalling molecule G protein subunit 11 (*GNG11*), as well as the SARS-CoV-2 early inflammation marker *IFI27*.[32,33] There was decreased expression of the placental marker Isthmin 2 (*ISM2*), potassium channels *KCNH3* and *KCNJ9*, and serotonin transporter *SLC6A4*.

Pathway enrichment analysis showed villous core stromal cells to be enriched with pathways related to increased oxidative stress, nitrosative stress, and methylglyoxal levels (cluster 1; Figure 6, B and C; Supplemental File 1 and 2). In parallel, systemic pressure, vasodilation, and hyperpolarisation related pathways were detected in cluster 17 (Figure 6, Bi and Bii). There was notable upregulation of immune related pathways and hypersensitivity in cluster 3 (Figure 6, B and C). Increases in collagen deposition, integrins, and TGF*β* were evident in clusters 18 and 22 (Figure 6, B and C). Increase in apolipoprotein E (*APOE*) clustered pathways related to lipid clearance in cluster 2. Among the downregulated clusters 1 and 7, there was downregulation of pathways related to various transport mechanisms, such as downregulation in potassium channels, acetylcholine, and serotonin transport pathways (Figure 6, D and E). Pathways related to reduced olfactory receptors were evident in cluster 2 (Figure 6, D and E) and decreased glucose detection in cluster 16 (Figure 6, D and E). Downregulation of several cytochromes P450 family 2 (CYP2) epoxygenase genes were present in cluster 14 (Figure 6, D and E) and downregulation of chemokine receptors was evident in cluster 3 (Figure 6, D and E).

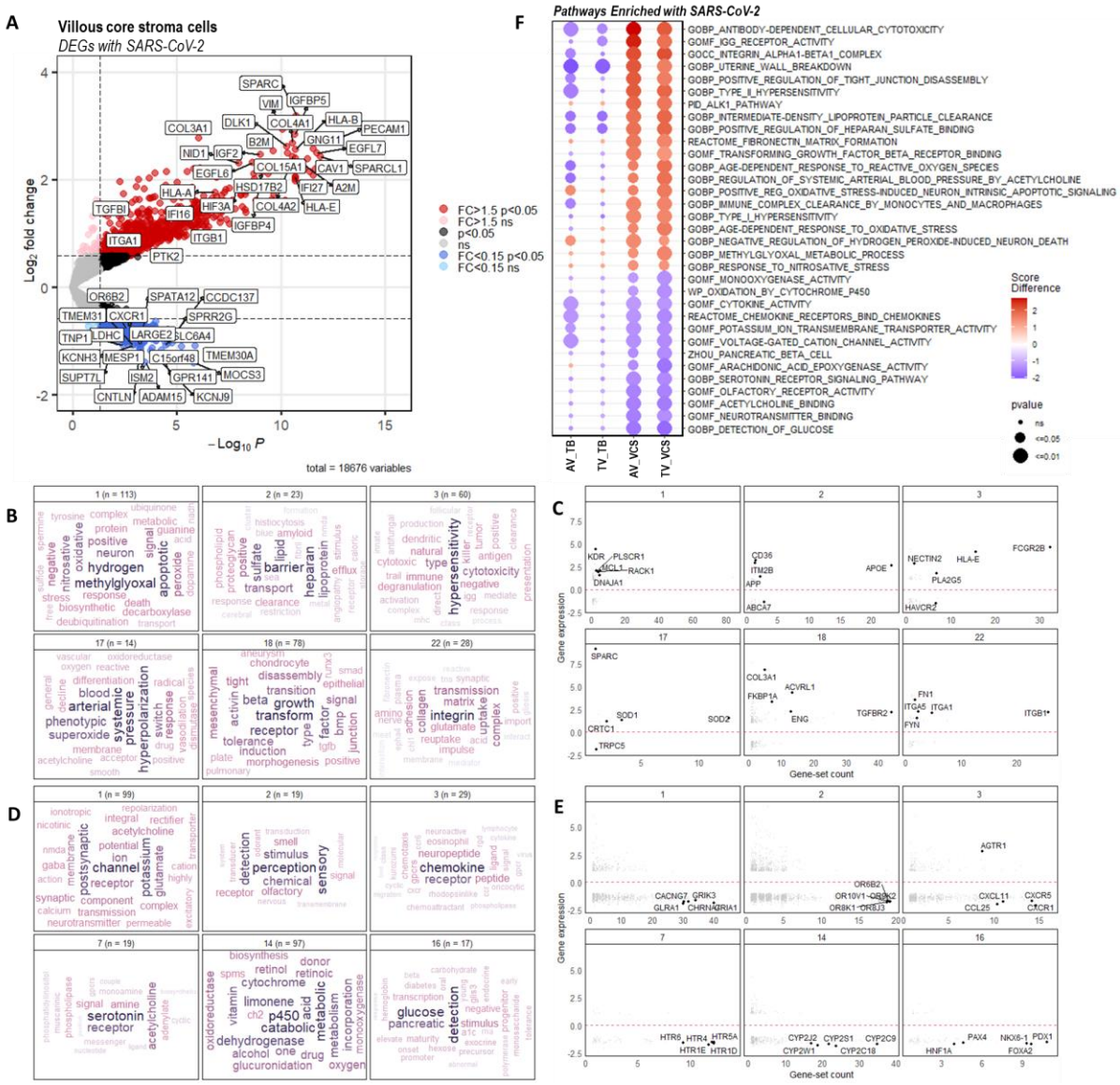

Figure 5: Response of villous core stroma cells to SARS-CoV-2. A*) Volcano plot of gene expression from villous core stroma cells in response to SARS-CoV-2. Fold change +/- 1.5, p-value <= 0.05.* ***B****) Select pathway clusters positively enriched in villous core stroma cells and* ***C****) the top 5 most common genes within each pathway cluster in C.* ***D****) Select pathway clusters negatively enriched in villous core stroma cells and* ***E****) the top 5 most common genes within each pathway cluster in D. Number of pathways within each pathway cluster is indicated at the top of each cluster box. Top 20 positively and negatively enriched pathway clusters can be found in Supplemental File 2.* ***F)*** *Enrichment score difference of select pathways from B and D in trophoblasts and villous core stroma cells at the anchoring and terminal villi. Full list of enriched pathways can be found in Supplemental File 1. Colour gradient refers to score difference in SARS-CoV-2 versus control samples; p-value <= 0.05. TB: trophoblasts, VCS: villus core stroma cells, AV: anchoring villi, TV: terminal villi, DEGs: differentially expressed genes.*

Discussion

To our knowledge, this is the first study examining the transcriptional response of histologically intact term-placental tissue to SARS-CoV-2. While our cohort is relatively small, and limited by its cross-sectional nature, through our study design we were able to elucidate the unique and cross-influential response of trophoblasts and villous core stroma cells at the anchoring and terminal villi of the placenta in response to SARS-CoV-2. Close

examination of the transcriptional alterations occurring in the trophoblast and villous core stroma cells in response to SARS-CoV-2 revealed a notable number of genes that are enriched in biological pathways previously associated with preeclampsia.

The trophoblast cells comprise the outer-most physical barrier of the placenta and are responsible for foetal-maternal nutrient and gas exchange, as well as metabolic and immunological functions in response to external stimuli.[34,35] In our study, we observed trophoblasts to transcriptionally respond to SARS-CoV-2 in a manner suggestive of supporting favourable foetal development with concurrent increase in compensatory mechanisms against hypertension and inflammation. For instance, several immunomodulatory pregnancy specific glycoproteins (*PSG1-9* and *PSG11)*, as well as genes from the Growth Hormone (GH) locus, (*GH1*; *GH2*, *CSH2*, *CSHL1*), were upregulated in trophoblasts in the SARS-CoV2 group compared to control. The expression of both gene families has been previously shown to naturally increase with term, supporting immune protection and nutrition of the foetus, where their additional increase in our SARS-CoV-2 dataset may suggest a natural protective mechanism against placental stress. [36-38] A number of studies suggest that PSGs can increase the expression and induce latent activation of the potent anti-inflammatory cytokine TGF*β* superfamily, where increased levels of TGF*β*-1 have been associated with preeclampsia-associated systemic inflammation. [39] Incidentally, we observed increased *TGFβ-1/2/3* expression in the villous core stroma cells in response to SARS-CoV-2, where alongside the increased number of CD68 positive macrophages and expression of several inflammation related markers (i.e., *IFI27*, *A2M*, *B2M*, *GNG11*, *PECAM1*) and immune pathways observed in our SARS-CoV-2 dataset (Figure 4 Bi cluster 4), suggests that the placenta is actively responding to inflammation in a compensatory manner. [39]

Trophoblasts from our SARS-CoV-2 group had significantly higher levels of *NOS3* and downregulation of Caveolin 1 (*CAV1*) compared to the control group. Both the upregulation of NOS3 and the down regulation of CAV1 are associated with increased endogenous production of the vasodilator nitric oxide, as a response to altered vascular reactivity, endothelial dysfunction, and hypertension.[40,41] Interestingly, NOS has been previously found to be highly upregulated to supraphysiological levels in animal models of infection-mediated inflammation during pregnancy, leading researchers to hypothesise that increased NOS may play a role in placental inflammation.[42-44] In response to increased NOS by the trophoblasts, the villous core stromal cells showed increased expression in biological pathways related to systemic pressure, vasodilation, and hyperpolarisation. This included the downregulation of olfactory receptors, potassium channels, and serotonin transporters, alongside upregulated hypoxia inducing factor 3A (*HIF3A*), suggesting deregulation of the vascular tone and blood pressure due to a hypoxic environment[45]. Further, there was downregulation of a number of cytochrome P450 family 2 (CYP2) epoxygenase genes, suggesting a decrease of arachidonic acid conversion into epoxyeicosatrienoic acids (EETs), which have downstream effects on hemodynamic adaptation of the placenta to hypertension.[46] In parallel, villous core stromal cells also showed enrichment of pathways related to oxidative stress, nitrosative stress, and increased methylglyoxal levels, all features associated with placental stress, and incidentally, preeclampsia.[47,48] Alongside, there was increased enrichment of the PI3K/AKT/mTOR pathway genes, where studies in a mouse model of preeclampsia support that its activation combats oxidative stress, suggesting the placenta actively responding to oxidative stress in a defensive manner.[23,24] The villous core stromal cells had notable upregulation of profibrotic osteonectin (SPARC), as well as several collagens and enrichment of collagen deposition pathways, suggestive of fibrosis, a common feature of preeclampsia.[49-51] This finding is in line with the more extensive histological evaluation of our cohort by a parallel study by Rebutini et al., where the SARS-Cov-2 cohort had increased deposition of villous fibrin compared to the control group.[17]

Additional transcriptional analysis of trophoblast and villous core stromal cells from SARS-CoV-2 samples identified several transcriptional variations that have been associated with preeclampsia. Trophoblasts had higher expression of *FLT1*, where excessive release of soluble FLT1 by syncytiotrophoblasts is a characteristic marker of late onset preeclampsia[13]. There was prominent increase of *PAPPA* and *PAPPA2* in the trophoblasts, the latter considered to become upregulated in response to placental pathologies, including preeclampsia.[52] Notably, the PAPPA2 substrates IGFB4 and IGFBP5 were concurrently upregulated in the villous core stromal cells, whereby the interaction of PAPPA2 with IGFBP4/5 has been shown to increase levels of IGF2, which was also increased in the villous core stroma cells in the SARS-CoV-2 group.[31] Additionally, the villous core stromal cells had increased levels of Isthmin-2 (*ISM1*), a placental marker associated with preeclampsia[53], as well as

apolipoprotein E (*APOE*) and pathways related to lipid clearance, which are also associated with preeclampsia [54,55]

Genes involved in synthesis and metabolism of steroid hormones (*HSD3B1*, *HSD17B1*, and *CYP19A1*) found upregulated in preeclampsia and gestational hypertension were also upregulated in SARS-CoV-2 trophoblasts.[25] Additionally, there was upregulation of *ALPP*, a plasma membrane-bound glycoprotein secreted by syncytiotrophoblasts, where marked elevation in the serum has been associated with adverse obstetric and perinatal outcomes including preterm labour and hypertensive disorders of pregnancy.[56] Alongside, *CGA*, *GDF15*, *TFPI-2*, and *CRH* genes were also upregulated in SARS-CoV-2 trophoblasts, all previously associated with placental oxidative stress, hypertension, and preeclampsia.[31,57-60] On the other hand, decrease in the expression of osteopontin, a factor involved in driving syncytiotrophoblast invasion and repair in preeclampsia-linked vascular injury, was also downregulated in SARS-CoV-2 trophoblast samples. Additionally, SARS-CoV-2 trophoblasts samples had decreased levels of complement component C1Q (*C1QA*/*B*/*C*) where its deficiency in pregnancy has been associated with impaired syncytiotrophoblast invasion and preeclampsia .[61,62] Coagulation factor XIII (*F13A1*), the last zymogen of the coagulation cascade that positively influences wound healing in several tissues, has been associated with pregnancy induced hypertension and preeclampsia and was also downregulated in SARS-CoV-2 trophoblasts.[63] Finally, DLK1, a protein where its downregulation has been associated with impaired response to metabolic demands during pregnancy and preeclampsia onset, was also downregulated in SARS-CoV-2 trophoblasts.[27,64]

In conclusion, our findings clearly highlight a differential expression suggesting that the placenta from pregnant participants with SARS-CoV-2 adopts a transcriptional profile aligning with stress responses observed in pregnant participants who develop preeclampsia. Using digital spatial profiling, our studies highlight the interplay between the trophoblast and villous core stroma cell populations, and how this crosstalk enriches pathways associated with preeclampsia. This study therefore sets a trajectory towards better understanding of "preeclampsia like syndrome" experienced by COVID-19 pregnant participants, uncovered using digital spatial profiling.

Acknowledgements

This study was funded by the Queensland University of Technology ECR funds for AK, JR, MA, NS. The following authors are supported by fellowships from the NHMRC (AK – 1157741, GB - 2008542 and 1135898), US DOD (NS – PC190533). The authors thank Fred Hutch pathology (Miki Haraguchi & Stephanie Weaver) for histology assistance.

Conflicts of Interest

Andy Nam and Liuliu Pan are employed by Nanostring Technologies. Nicolas Matigian is employed by QCIF Bioinformatics.

References

1 Bordt, E. A. *et al.* Maternal SARS-CoV-2 infection elicits sexually dimorphic placental immune responses. *Sci Transl Med* **13**, eabi7428, doi:10.1126/scitranslmed.abi7428 (2021).

2 Edlow, A. G. *et al.* Assessment of Maternal and Neonatal SARS-CoV-2 Viral Load, Transplacental Antibody Transfer, and Placental Pathology in Pregnancies During the COVID-19 Pandemic. *JAMA Netw Open* **3**, e2030455, doi:10.1001/jamanetworkopen.2020.30455 (2020).

3 Schwartz, D. A., Mulkey, S. B. & Roberts, D. J. SARS-CoV-2 Placentitis, Stillbirth and Maternal COVID-19 Vaccination: Clinical-Pathological Correlations. *Am J Obstet Gynecol*, doi:10.1016/j.ajog.2022.10.001 (2022).

4 Palomo, M. *et al.* Differences and similarities in endothelial and angiogenic profiles of preeclampsia and COVID-19 in pregnancy. *Am J Obstet Gynecol* **227**, 277 e271-277 e216, doi:10.1016/j.ajog.2022.03.048 (2022).

5 Mendoza, M. *et al.* Pre-eclampsia-like syndrome induced by severe COVID-19: a prospective observational study. *Bjog* **127**, 1374-1380, doi:10.1111/1471-0528.16339 (2020).

6 Serrano, B. *et al.* Confirmation of preeclampsia-like syndrome induced by severe COVID-19: an observational study. *Am J Obstet Gynecol MFM* **5**, 100760, doi:10.1016/j.ajogmf.2022.100760 (2022).

7 Naeh, A., Berezowsky, A., Yudin, M. H., Dhalla, I. A. & Berger, H. Preeclampsia-Like Syndrome in a Pregnant Patient With Coronavirus Disease 2019 (COVID-19). *J Obstet Gynaecol Can* **44**, 193-195, doi:10.1016/j.jogc.2021.09.015 (2022).

8 Prabhu, M. *et al.* Pregnancy and postpartum outcomes in a universally tested population for SARS-CoV-2 in New York City: a prospective cohort study. *Bjog* **127**, 1548-1556, doi:10.1111/1471-0528.16403 (2020).

9 Schwartz, D. A. *et al.* Placental Tissue Destruction and Insufficiency From COVID-19 Causes Stillbirth and Neonatal Death From Hypoxic-Ischemic Injury. *Arch Pathol Lab Med* **146**, 660-676, doi:10.5858/arpa.2022-0029-SA (2022).

10 Huang, C. *et al.* Clinical features of patients infected with 2019 novel coronavirus in Wuhan, China. *The Lancet* **395**, 497-506, doi:https://doi.org/10.1016/S0140-6736(20)30183-5 (2020).

11 Rasmussen, M. *et al.* RNA profiles reveal signatures of future health and disease in pregnancy. *Nature* **601**, 422-427, doi:10.1038/s41586-021-04249-w (2022).

12 Burton, G. J., Redman, C. W., Roberts, J. M. & Moffett, A. Pre-eclampsia: pathophysiology and clinical implications. *BMJ* **366**, l2381, doi:10.1136/bmj.l2381 (2019).

13 Roberts, J. M. *et al.* Subtypes of Preeclampsia: Recognition and Determining Clinical Usefulness. *Hypertension* **77**, 1430-1441, doi:10.1161/HYPERTENSIONAHA.120.14781 (2021).

14 Redman, C. W. & Staff, A. C. Preeclampsia, biomarkers, syncytiotrophoblast stress, and placental capacity. *Am J Obstet Gynecol* **213**, S9 e1, S9-11, doi:10.1016/j.ajog.2015.08.003 (2015).

15 Maltepe, E. & Fisher, S. J. Placenta: the forgotten organ. *Annu Rev Cell Dev Biol* **31**, 523-552, doi:10.1146/annurev-cellbio-100814-125620 (2015).

16 Buchrieser, J. *et al.* IFITM proteins inhibit placental syncytiotrophoblast formation and promote fetal demise. *Science* **365**, 176-180, doi:10.1126/science.aaw7733 (2019).

17 Rebutini, P. Z. *et al.* Association Between COVID-19 Pregnant Women Symptoms Severity and Placental Morphologic Features. *Front Immunol* **12**, 685919, doi:10.3389/fimmu.2021.685919 (2021).

18 Risso, D., Ngai, J., Speed, T. P. & Dudoit, S. Normalization of RNA-seq data using factor analysis of control genes or samples. *Nat Biotechnol* **32**, 896-902, doi:10.1038/nbt.2931 (2014).

19 Ritchie, M. E. *et al.* limma powers differential expression analyses for RNA-sequencing and microarray studies. *Nucleic Acids Res* **43**, e47, doi:10.1093/nar/gkv007 (2015).

20 Hanzelmann, S., Castelo, R. & Guinney, J. GSVA: gene set variation analysis for microarray and RNA-seq data. *BMC Bioinformatics* **14**, 7, doi:10.1186/1471-2105-14-7 (2013).

21 Dharmesh D. Bhuva, C. W. T., Ning Liu, Holly J. Whitfield, Nicholas Papachristos, Sam Lee, Malvika Kharbanda, Ahmed Mohamed, Melissa J. Davis. vissE: A versatile tool to identify and visualise higher-order molecular phenotypes from functional enrichment analysis. *bioRxiv* doi:https://doi.org/10.1101/2022.03.06.483195 (2022).

22 Aouache, R., Biquard, L., Vaiman, D. & Miralles, F. Oxidative Stress in Preeclampsia and Placental Diseases. *Int J Mol Sci* **19**, doi:10.3390/ijms19051496 (2018).

23 Yuan, Y. *et al.* SRC-3 Plays a Critical Role in Human Umbilical Vein Endothelial Cells by Regulating the PI3K/Akt/mTOR Pathway in Preeclampsia. *Reprod Sci* **25**, 748-758, doi:10.1177/1933719117725818 (2018).

24 He, C. *et al.* Hypoxia-induced Downregulation of SRC-3 Suppresses Trophoblastic Invasion and Migration Through Inhibition of the AKT/mTOR Pathway: Implications for the Pathogenesis of Preeclampsia. *Sci Rep* **9**, 10349, doi:10.1038/s41598-019-46699-3 (2019).

25 Shimodaira, M. *et al.* Estrogen synthesis genes CYP19A1, HSD3B1, and HSD3B2 in hypertensive disorders of pregnancy. *Endocrine* **42**, 700-707, doi:10.1007/s12020-012-9699-7 (2012).

26 Neill, T. *et al.* Decorin antagonizes the angiogenic network: concurrent inhibition of Met, hypoxia inducible factor 1alpha, vascular endothelial growth factor A, and induction of thrombospondin-1 and TIMP3. *J Biol Chem* **287**, 5492-5506, doi:10.1074/jbc.M111.283499 (2012).

27 Pittaway, J. F. H., Lipsos, C., Mariniello, K. & Guasti, L. The role of delta-like non-canonical Notch ligand 1 (DLK1) in cancer. *Endocr Relat Cancer* **28**, R271-R287, doi:10.1530/ERC-21-0208 (2021).

28 Chiu, Y. H. & Chen, H. GATA3 inhibits GCM1 activity and trophoblast cell invasion. *Sci Rep* **6**, 21630, doi:10.1038/srep21630 (2016).

29 Sutton, E. F., Gemmel, M. & Powers, R. W. Nitric oxide signaling in pregnancy and preeclampsia. *Nitric Oxide* **95**, 55-62, doi:10.1016/j.niox.2019.11.006 (2020).

30 Cao, C. & Fleming, M. D. The placenta: the forgotten essential organ of iron transport. *Nutr Rev* **74**, 421-431, doi:10.1093/nutrit/nuw009 (2016).

31 Nishizawa, H. *et al.* Increased levels of pregnancy-associated plasma protein-A2 in the serum of pre-eclamptic patients. *Mol Hum Reprod* **14**, 595-602, doi:10.1093/molehr/gan054 (2008).

32 Kulasinghe, A. *et al.* Profiling of lung SARS-CoV-2 and influenza virus infection dissects virus-specific host responses and gene signatures. *Eur Respir J* **59**, doi:10.1183/13993003.01881-2021 (2022).

33 Du, R., Li, L. & Wang, Y. N6-Methyladenosine-Related Gene Signature Associated With Monocyte Infiltration Is Clinically Significant in Gestational Diabetes Mellitus. *Front Endocrinol (Lausanne)* **13**, 853857, doi:10.3389/fendo.2022.853857 (2022).

34 Gohner, C., Plosch, T. & Faas, M. M. Immune-modulatory effects of syncytiotrophoblast extracellular vesicles in pregnancy and preeclampsia. *Placenta* **60 Suppl 1**, S41-S51, doi:10.1016/j.placenta.2017.06.004 (2017).

35 Lager, S. & Powell, T. L. Regulation of nutrient transport across the placenta. *J Pregnancy* **2012**, 179827, doi:10.1155/2012/179827 (2012).

36 Grudzinskas, J. G. *et al.* Identification of high-risk pregnancy by the routine measurement of pregnancy-specific beta 1-glycoprotein. *Am J Obstet Gynecol* **147**, 10-12, doi:10.1016/0002-9378(83)90075-3 (1983).

37 Liao, S., Vickers, M. H., Stanley, J. L., Baker, P. N. & Perry, J. K. Human Placental Growth Hormone Variant in Pathological Pregnancies. *Endocrinology* **159**, 2186-2198, doi:10.1210/en.2018-00037 (2018).

38 Iacob, D. *et al.* Decorin-mediated inhibition of proliferation and migration of the human trophoblast via different tyrosine kinase receptors. *Endocrinology* **149**, 6187-6197, doi:10.1210/en.2008-0780 (2008).

39 Liu, L. Y. *et al.* Integrating multiple 'omics' analyses identifies serological protein biomarkers for preeclampsia. *BMC Med* **11**, 236, doi:10.1186/1741-7015-11-236 (2013).

40 Mistry, H. D. *et al.* Differential placental caveolin-1 gene expression in women with pre-eclampsia. *Archives of Disease in Childhood - Fetal and Neonatal Edition* **96**, Fa125-Fa126 (2011).

41 Mukosera, G. T. *et al.* Nitric oxide metabolism in the human placenta during aberrant maternal inflammation. *J Physiol* **598**, 2223-2241, doi:10.1113/JP279057 (2020).

42 Nowicki, B., Singhal, J., Fang, L., Nowicki, S. & Yallampalli, C. Inverse relationship between severity of experimental pyelonephritis and nitric oxide production in C3H/HeJ mice. *Infect Immun* **67**, 2421-2427, doi:10.1128/iai.67.5.2421-2427.1999 (1999).

43 Ogando, D. G., Paz, D., Cella, M. & Franchi, A. M. The fundamental role of increased production of nitric oxide in lipopolysaccharide-induced embryonic resorption in mice. *Reproduction* **125**, 95-110, doi:10.1530/rep.0.1250095 (2003).

44 Kong, L. *et al.* Polarization of macrophages induced by Toxoplasma gondii and its impact on abnormal pregnancy in rats. *Acta Trop* **143**, 1-7, doi:10.1016/j.actatropica.2014.12.001 (2015).

45 Wareing, M. *et al.* Expression and function of potassium channels in the human placental vasculature. *Am J Physiol Regul Integr Comp Physiol* **291**, R437-446, doi:10.1152/ajpregu.00040.2006 (2006).

46 Jiang, H. *et al.* Maternal and fetal epoxyeicosatrienoic acids in normotensive and preeclamptic pregnancies. *Am J Hypertens* **26**, 271-278, doi:10.1093/ajh/hps011 (2013).

47 Sankaralingam, S., Xu, H., Jiang, Y., Sawamura, T. & Davidge, S. T. Evidence for increased methylglyoxal in the vasculature of women with preeclampsia: role in upregulation of LOX-1 and arginase. *Hypertension* **54**, 897-904, doi:10.1161/HYPERTENSIONAHA.109.135228 (2009).

48 Afrose, D. *et al.* The diagnostic potential of oxidative stress biomarkers for preeclampsia: systematic review and meta-analysis. *Biol Sex Differ* **13**, 26, doi:10.1186/s13293-022-00436-0 (2022).

49 Tossetta, G. *et al.* Pre-eclampsia onset and SPARC: A possible involvement in placenta development. *J Cell Physiol* **234**, 6091-6098, doi:10.1002/jcp.27344 (2019).

50 Kos, K. *et al.* Regulation of the fibrosis and angiogenesis promoter SPARC/osteonectin in human adipose tissue by weight change, leptin, insulin, and glucose. *Diabetes* **58**, 1780-1788, doi:10.2337/db09-0211 (2009).

51 Richards, C. *et al.* Characterisation of cardiac health in the reduced uterine perfusion pressure model and a 3D cardiac spheroid model, of preeclampsia. *Biol Sex Differ* **12**, 31, doi:10.1186/s13293-021-00376-1 (2021).

52 Wagner, P. K., Otomo, A. & Christians, J. K. Regulation of pregnancy-associated plasma protein A2 (PAPPA2) in a human placental trophoblast cell line (BeWo). *Reprod Biol Endocrinol* **9**, 48, doi:10.1186/1477-7827-9-48 (2011).

53 Martinez, C. *et al.* Isthmin 2 is decreased in preeclampsia and highly expressed in choriocarcinoma. *Heliyon* **6**, e05096, doi:10.1016/j.heliyon.2020.e05096 (2020).

54 Khedun, S. M., Naicker, T., Moodley, J. & Gathiram, P. Urinary heparan sulfate proteoglycan excretion in black African women with pre-eclampsia. *Acta Obstet Gynecol Scand* **81**, 308-312, doi:10.1034/j.1600-0412.2002.810405.x (2002).

55 Chen, H. *et al.* Maternal plasma proteome profiling of biomarkers and pathogenic mechanisms of early-onset and late-onset preeclampsia. *Sci Rep* **12**, 19099, doi:10.1038/s41598-022-20658-x (2022).

56 Lozo, S., Atabeygi, A. & Healey, M. Extreme Elevation of Alkaline Phosphatase in a Pregnancy Complicated by Gestational Diabetes and Infant with Neonatal Alloimmune Thrombocytopenia. *Case Rep Obstet Gynecol* **2016**, 4896487, doi:10.1155/2016/4896487 (2016).

57 Sugulle, M. *et al.* Circulating and placental growth-differentiation factor 15 in preeclampsia and in pregnancy complicated by diabetes mellitus. *Hypertension* **54**, 106-112, doi:10.1161/HYPERTENSIONAHA.109.130583 (2009).

58 Hogg, K., Blair, J. D., McFadden, D. E., von Dadelszen, P. & Robinson, W. P. Early onset pre-eclampsia is associated with altered DNA methylation of cortisol-signalling and steroidogenic genes in the placenta. *PLoS One* **8**, e62969, doi:10.1371/journal.pone.0062969 (2013).

59 Zheng, L. *et al.* Overexpression of tissue factor pathway inhibitor 2 attenuates trophoblast proliferation and invasion in preeclampsia. *Hum Cell* **33**, 512-520, doi:10.1007/s13577-020-00322-0 (2020).

60 Bralewska, M. *et al.* Chromogranin A demonstrates higher expression in preeclamptic placentas than in normal pregnancy. *BMC Pregnancy Childbirth* **21**, 680, doi:10.1186/s12884-021-04139-z (2021).

61 Xia, J., Qiao, F., Su, F. & Liu, H. Implication of expression of osteopontin and its receptor integrin alphanubeta3 in the placenta in the development of preeclampsia. *J Huazhong Univ Sci Technolog Med Sci* **29**, 755-760, doi:10.1007/s11596-009-0617-z (2009).

62 Singh, J., Ahmed, A. & Girardi, G. Role of complement component C1q in the onset of preeclampsia in mice. *Hypertension* **58**, 716-724, doi:10.1161/HYPERTENSIONAHA.111.175919 (2011).

63 Ebina, Y. *et al.* O127. Low levels of plasma protein S, protein C and coagulation factor XII during early pregnancy and adverse pregnancy outcome. *Pregnancy Hypertension: An International Journal of Women's Cardiovascular Health* **5**, 239-240, doi:https://doi.org/10.1016/j.preghy.2015.07.077 (2015).

64 Schrey, S. *et al.* The adipokine preadipocyte factor-1 is downregulated in preeclampsia and expressed in placenta. *Cytokine* **75**, 338-343, doi:10.1016/j.cyto.2015.07.021 (2015).